

DESIGN STUDIES ON AN S-BAND HYBRID ACCELERATING STRUCTURE*

B. Gao†, S. Pei, Y. Chi, Key Laboratory of Particle Acceleration Physics and Technology, Institute of High Energy Physics, Chinese Academy of Science, Beijing, China

Abstract

In an electron linac, the composition of the bunching system is determined by the synthetical consideration of the beam performance and the construction cost. In the industrial area, the bunching system is usually simplified to reduce the construction cost by eliminating the PB and integrating the B and the standard accelerating structure to form the β -varied structure. The bunching performance for this kind of system is relatively worse than that for the standard one. To keep the beam performance of the standard bunching system and reduce the construction cost as much as possible, the HAS is proposed by integrating the PB, the B and the standard TW accelerating structure together. The HAS can be widely applied in the industrial area to enhance the beam performance of the industrial linac but not increase the cost. In this paper, the design studies on an S-band (2856 MHz) HAS is presented. The HAS studied here is composed of 2 SW cells, 40 TW cells and 2 coupler cells. The on-axis electric field amplitude distribution simulated by HFSS can fully meet the beam dynamics requirement.

INTRODUCTION

The standard bunching system consists of a standing wave (SW) prebuncher (PB), a traveling wave (TW) buncher (B) and a TW accelerating structure in an electron liner accelerator. Inspired by the ingenious idea of the hybrid photo-injector developed by the INFN-LNF/UCLA/ SAPIENZA collaboration [1], we successfully built the hybrid buncher (HB) [2]. It has been proved that the HB is an innovative attempt to reduce the construction cost of the standard bunching system but preserve the beam quality as much as possible [3]. In this scenario, to exclusively simplify the standard bunching system, the hybrid accelerating structure (HAS) shown in Fig. 1 is proposed by integrating the PB, the B and the standard accelerating structure together [4]. Compared to the standard bunching system, the one with the HAS is more compact, and the cost is lowered to the largest extent without fairly degrading the beam performance.

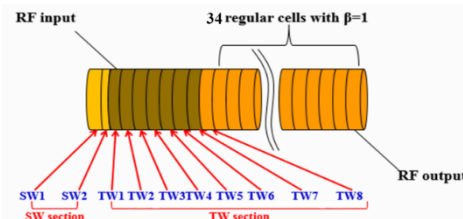


Figure 1: The schematic layout of the HAS.

Supported by the National Natural Science Foundation of China and the Youth Innovation Promotion Association of Chinese Academy of Sciences, China, we are building an S-band (2856 MHz) HAS prototype. The HAS prototype is composed of 2 SW cells, 40 TW cells and 2 coupler cells. The 2 SW cells operate at $\pi/2$ mode, while the 40 TW cells operate at $2\pi/3$ mode. The SW section of the HAS is generally the same as that of the HB [2, 3], while the iris apertures between the SW cells and the input RF coupler cell need to be adjusted carefully to obtain the appropriate field distribution. Beam dynamics study on the bunching system with the HAS has been done, it is shown that the HAS bunching system can keep the beam performance of the standard one as much as possible [4].

In this paper, the RF design of the HAS prototype is presented. Initially, 2D code SUPERFISH [5] was used to determine the dimensions of all the cells. Secondly, 3D code HFSS [6] was used to optimize the input and output RF coupler cells. Finally, the on-axis RF field distribution of the whole HAS prototype was calculated, which can fully meet the beam dynamics requirement determined by PARMELA [7].

INITIAL 2D DESIGN

The initial 2D design for the SW and the TW sections of the HAS were performed separately in SUPERFISH by setting appropriate boundary conditions and material properties. Table 1 lists the basic design requirement of the HAS [4],

In the TW section, the 1st and 42nd cells correspond to the RF input and output coupler cells respectively. The 2nd to 6th are β -varied cells and the rests are regular cells.

*Work supported by the National Natural Science Foundation of China (11475201) and the Youth Innovation Promotion Association of Chinese Academy of Sciences, China.

† email address: gaobin@ihep.ac.cn.

Table 1: The Basic Design Requirement of the HAS

Section	Cell #	β	Cell length [mm]
SW section	1	0.94	32.80
	2	0.56	19.68
	1	0.75	26.24
TW section	2	0.75	26.24
	3	0.75	26.24
	4	0.88	30.79
	5	0.92	32.19
	6	0.95	33.24
	7~42	1	34.98

TW Section Design

The TW section is the traditional disk-loaded type waveguide structure, which operates at $2\pi/3$ mode. By using the SUPERFISH model shown in Fig. 2, the RF characteristics (frequency f , quality factor Q , shunt impedance r_0 , group velocity v_g/c , etc) of each cell are calculated. Finally, by colligating all the calculated results for the TW cells together, the main specifications for the TW section listed in Table 2 can be obtained.

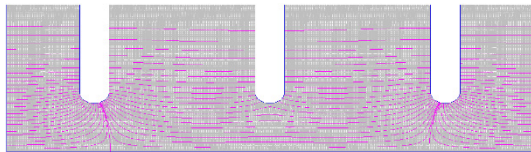


Figure 2: The 2D SUPERFISH model for the TW cells.

Table 2: The Main Specifications of the TW Section

Parameters	Value
Frequency f [MHz]	2856
Operating temperature [°C]	35 ± 0.1
Number of cells	40
Phase advance per cell [°]	120
Cell length [mm]	26.24~34.98
Disc thickness [mm]	5.843
Iris diameter $2a$ [mm]	28.52~23.73
Cell diameter $2b$ [mm]	85.47~82.77
Shunt impedance r_0 [M Ω /m]	28.36~57.05
Quality factor Q	10980~13753
Group velocity v_g/c	0.0246~0.0141
Filling time [ns]	239
Attenuation coefficient [Np]	0.16

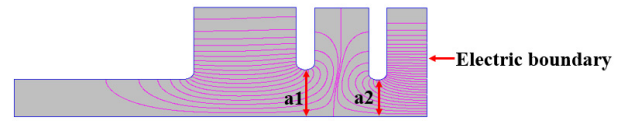


Figure 3: The 2D SUPERFISH model for the SW section.

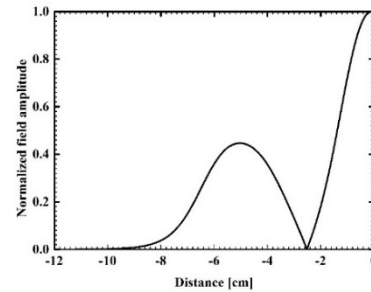


Figure 4: The field amplitude distribution along the axis of the SW section.

SW Section Design

It is well known that half of the coupler cell in the TW accelerating structure operates at the SW mode, thus by using the SUPERFISH model shown in Fig. 3 the SW section of the HAS can be designed and optimized. The left two cells are the 2 SW cells of the HAS, while the right half-cell corresponds to the input RF coupler cell. By tuning the dimensions of a_1 and a_2 , the field amplitude ratio between the SW and the TW sections can be changed.

Figure 4 shows the optimized electric field amplitude distribution along the axis of the SW section. The ratio of the value for the 1st peak to that for the 2nd peak is ~ 0.45 , which is $\sim 4\%$ smaller than the optimized value of ~ 0.47 [4]. Due to the existence of simulation and fabrication errors, this small deviation is within the tolerance and can be acceptance.

3D DESIGN OF THE HAS

The 2D RF design of the HAS is the starting point of the 3D design. Similarly, the SW and the TW sections of the HAS are designed separately.

There may be some frequency difference between the 2D and the 3D simulations. To recover the resonate frequency of each cell back to the nominal value of 2856 MHz, the cell diameter of each cell needs to be adjusted in the 3D simulation. However, all the other dimensions of each cell determined by 2D simulation should be fixed.

Coupler Design

Both the input and output RF couplers can be designed based on the matching procedure for the $2\pi/3$ structure proposed by Dr. R. L. Kyhl and confirmed with the field transmission method. However, for the input coupler, attachment of the SW section with the TW section will change the coupler matching status. Fortunately, it has been proved that the power dissipation in the SW section is much smaller than the power transmitted to the TW section [3]. Therefore, when the field transmission method is used to confirm the input RF coupler matching status,

Content from this work may be used under the terms of the CC BY 3.0 licence (© 2017). Any distribution of this work must maintain attribution to the author(s), title of the work, publisher, and DOI.

only minor modification of the dimensions for the coupler cell is needed. Table 3 shows the matching results of the input RF coupler based on the Kyhl method. Fig. 5 shows the 3D HFSS model of the RF input coupler based on the transmission method. By slightly tuning the cavity size and the coupling iris width of the coupler cavity, the S11 curve shown in Fig. 6 can be obtained. The S11 value at the operating frequency 2856 MHz is ~ -40 dB, which means the matching of the input RF coupler is very well.

Table 3: The Matching Results of the Input RF Coupler

Frequency [MHz]	Phase I [°]	Phase II [°]	Phase rotation [°]	β & Δf [MHz]
2829.7	57.4	-62.4	119.8	
2842.8	51.0	-130	181.0	1.01 & -0.04
2856.0	44.7	164	240.7	

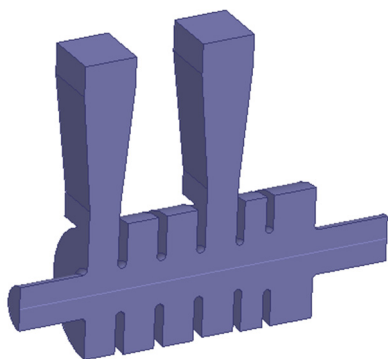


Figure 5: The 3D HFSS model of the input RF coupler based on the transmission method.

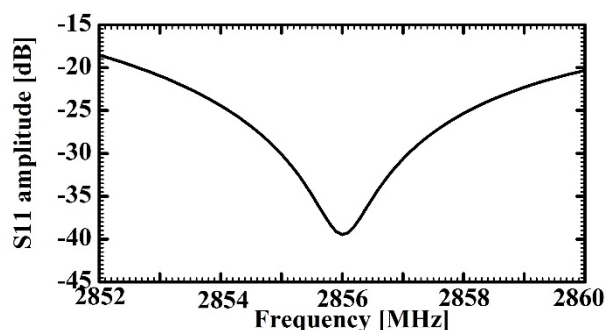


Figure 6: The S11 curve for the input RF coupler.

Design of the Whole Structure

By assembling the SW section, the TW section and the two RF couplers together, the 3D structure of the HAS can be determined and constructed.

In recent years, with the development of the computer technology, simulation of the full 3D structure of the HAS becomes possible. In this situation, calculation of the HAS was carried out in HFSS. To minimize the CPU time and the memory use, only 1/2 model of the HAS shown in Fig. 7 was created and simulated by setting appropriate boundary conditions.

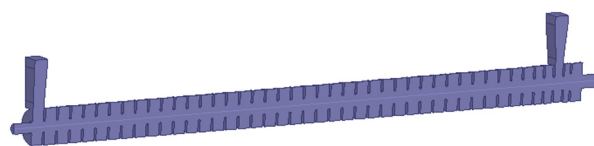


Figure 7: The 1/2 model of the HAS created in HFSS.

Figure 8 shows the electric field amplitude distribution along the axis of the HAS. For comparison, the field distribution used in PARMELA is also shown. One can see that there are 43 peaks, 1st of which corresponds to the 1st cell in the SW section. The 2nd and 43rd peaks correspond to the input and output couplers, respectively. The other 40 peaks correspond to the 40 TW cells. The HFSS simulation result is consistent with the beam dynamics requirement. Figure 9 shows the electric field phase distribution along the axis of the HAS. The phase jump between the SW and the TW sections is 180°, which indicates the operating mode in the SW section is $\pi/2$ mode. In the TW section, the phase advance from one cell to another is 120°, which is the case of $2\pi/3$ mode.

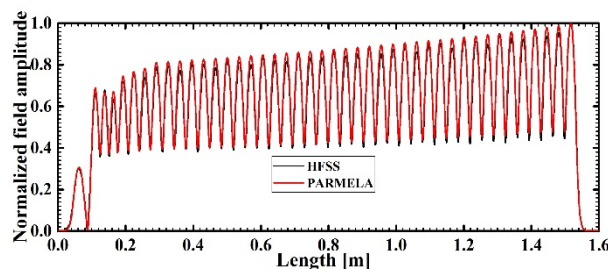


Figure 8: The electric field amplitude distribution along the axis of the HAS.

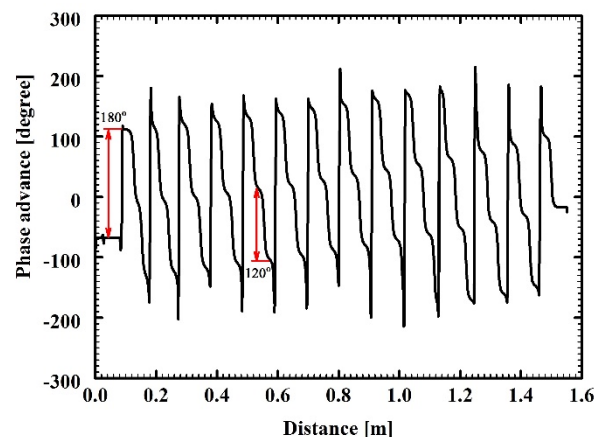


Figure 9: The electric field phase distribution along the axis of the HAS.

CONCLUSION

The RF design studies on the HAS has been conducted by SUPERFISH and HFSS. The obtained distribution can fully meet the beam dynamics requirement. The HAS combines the functions of the PB, the B and the standard TW accelerating structure, it can be widely applied in the industrial area.

REFERENCES

- [1] D. Alesini *et al.*, The Design of a Hybrid Photon Injector for High Brightness Beam Applications, in *Proc. EPAC2006*, Edinburgh, Scotland, 2006, WEPLS048, p.2487.
- [2] S. Zhao *et al.*, Field Distribution Measurement and Tuning of the Hybrid Buncher, *High Power Laser and Particle Beams*, 2017, 29(6): 065104.
- [3] S. Pei *et al.*, Studies on an S-band Bunching System with Hybrid Buncher, *Chinese Physics C*, 2013, 37(11): 117001.
- [4] S. Pei *et al.*, Studies on the S-band Bunching System with the Hybrid Accelerating Structure, presented at *SAP2017*, this proceedings, paper MOPH23.
- [5] J. Billen *et al.*, POSSION SUPERFISH, LA-UR-96-1834, LANL, 2006.
- [6] HFSS, www.ansys.com
- [7] L. Young *et al.*, PARMELA. LA-UR-96-1835, LANL, 2005.